

AD-A148 159

QUANTUM MONTE CARLO FOR MOLECULES(U) CALIFORNIA UNIV
BERKELEY LAWRENCE BERKELEY LAB W A LESTER ET AL.
01 NOV 84 N00014-83-F-0101

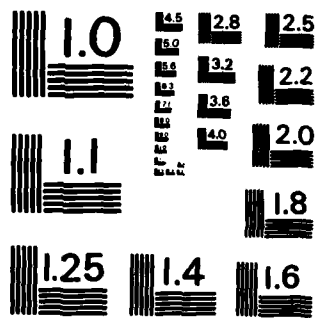
1/1

UNCLASSIFIED

F/G 20/10

NL





MICROCOPY RESOLUTION TEST CHART
NATIONAL BUREAU OF STANDARDS-1963-A

Unclassified

12

SECURITY CLASSIFICATION OF THIS PAGE (When Data Entered)

REPORT DOCUMENTATION PAGE		READ INSTRUCTIONS BEFORE COMPLETING FORM
1. REPORT NUMBER	2. GOVT ACCESSION NO.	3. RECIPIENT'S CATALOG NUMBER
4. TITLE (and Subtitle) ANNUAL SUMMARY REPORT QUANTUM MONTE CARLO FOR MOLECULES		5. TYPE OF REPORT & PERIOD COVERED Annual Summary Report 1/1/84 through 12/31/84
7. AUTHOR(s) William A. Lester, Jr. and Peter J. Reynolds		6. PERFORMING ORG. REPORT NUMBER
9. PERFORMING ORGANIZATION NAME AND ADDRESS Materials and Molecular Research Division, Lawrence Berkeley Laboratory, University of California, Berkeley, California 94720		8. CONTRACT OR GRANT NUMBER(s) N00014-83-F-0101
11. CONTROLLING OFFICE NAME AND ADDRESS Office of Naval Research, Physics Division Office (Code 412) 800 North Quincy Street, Arlington, Virginia 22217		10. PROGRAM ELEMENT, PROJECT, TASK AREA & WORK UNIT NUMBERS 61153N, RR011-03-05, NR 602-011
14. MONITORING AGENCY NAME & ADDRESS (if different from Controlling Office)		12. REPORT DATE 1 November 1984
		13. NUMBER OF PAGES 19
		15. SECURITY CLASS. (of this report) Unclassified
		15a. DECLASSIFICATION/DOWNGRADING SCHEDULE
16. DISTRIBUTION STATEMENT (of this Report) Approved for public release; distribution unlimited.		
17. DISTRIBUTION STATEMENT (of the abstract entered in Block 20, if different from Report)		
18. SUPPLEMENTARY NOTES		
19. KEY WORDS (Continue on reverse side if necessary and identify by block number) Quantum Monte Carlo importance functions nitrogen molecules reaction barrier binding energy theoretical excited states fluorine electronic structure methylene electron affinity Schrödinger equation parallel computation		
20. ABSTRACT (Continue on reverse side if necessary and identify by block number) Research progress on an alternative method to variational and perturbative approaches for the electronic structure of molecules is described. Advances including (1) the first computation of a molecular excited state (CH ₂) and (2) best computed bound to the classical barrier to the hydrogen exchange reaction are described.		

AD-A148 159

DTIC FILE COPY

DTIC
ELECTE
DEC 03 1984
S E

DD FORM 1473 1 JAN 73

EDITION OF 1 NOV 68 IS OBSOLETE
S/N 0102-LF-014-6601

Unclassified
SECURITY CLASSIFICATION OF THIS PAGE (When Data Entered)

84 11 26 08 9

OFFICE OF NAVAL RESEARCH

ANNUAL SUMMARY REPORT

for

1 January 1984 through 31 December 1984

for

Contract N00014-83-F-0101

Task No. RR011-03-0D

QUANTUM MONTE CARLO FOR MOLECULES

William A. Lester, Jr.

Peter J. Reynolds

Materials and Molecular Research Division

Lawrence Berkeley Laboratory

University of California

Berkeley, California 94720

Accession For	
NTIS GRA&I	<input checked="" type="checkbox"/>
DTIC TAB	<input type="checkbox"/>
Unannounced	<input type="checkbox"/>
Justification	
By _____	
Distribution/	
Availability Codes	
Dist	Avail and/or Special
A-1	



ANNUAL SUMMARY REPORT

"Quantum Monte Carlo for Molecules"

Principal Investigators:

William A. Lester, Jr.

Peter J. Reynolds

Materials and Molecular Research Division
Lawrence Berkeley Laboratory
University of California
Berkeley, California 94720

Description of Problem and Approach

Monte Carlo approaches to solving problems with many degrees of freedom are a class of statistical methods having in common the generation of "random" numbers. In the past few years, Monte Carlo approaches have seen increased application in a number of diverse fields. In particular, quantum mechanical Monte Carlo (QMC) methods¹⁻¹³ have been successfully used for the treatment of molecular problems^{3,5,8-12}. What we mean here by QMC is a Monte Carlo procedure which solves the Schrödinger equation. This is to be distinguished from so-called variational Monte Carlo, in which one obtains expectation values for a *given* trial wave function.

This ability to stochastically solve the Schrödinger equation provides an alternative to conventional techniques of quantum chemistry. Early work⁸ has shown that highly accurate total energies and correlation energies can be obtained by QMC. In fact, in a procedurally simple manner, accuracies exceeding those of the best *ab initio* configuration interaction calculations have been obtained.

Much of chemistry takes place predominantly in the valence electrons of a system. Thus the quantities of interest are usually small differences of large total energies. If QMC is to be useful in calculating binding energies, affinities, reaction barriers, etc., it needs not only to be able to calculate accurate *total* energies, but also these more relevant energy *differences*. This is a far more difficult task for Monte Carlo, since a statistical uncertainty of as little as 0.1% in

the separate total energies can mask the sought-after energy difference. To reduce the statistical error to the level needed by "brute force" is costly in computer time, as the standard deviation decreases only as $(CPU\ time)^{-1/2}$. Algorithmic developments, such as differential QMC¹⁴, hold promise for reductions in variance through correlated sampling techniques. Another approach is based on noting that the variance decreases as Ψ_T better approximates the true eigenfunction. To take advantage of this we have developed an iterative procedure for improving Ψ_T . We describe this approach in the next section.

Also under development is the use of pseudo-potentials in QMC to describe the core electrons; in this way only the valence electrons need to be involved in the QMC calculation. One wants also to be able to use QMC to calculate potential energy surfaces, excited states, dipole moments, and other molecular properties. Research is continuing along these lines. We describe in the next section some of the results we have obtained. Among these results is the first calculation of an excited state energy by Monte Carlo. Before going into more detail, in what follows we describe the actual QMC approach.

Briefly, the procedure is to simulate the quantum system by allowing it to evolve under the time-dependent Schrödinger equation in imaginary time. It is easy to show⁶ that the use of imaginary time causes the system to approach a stationary state which is the lowest state of a given symmetry. Properties may then be "measured" as averages over the resulting equilibrium distribution.

By writing the imaginary-time Schrödinger equation with a shift in the zero of energy as

$$\frac{\partial \Psi(\underline{R}, t)}{\partial t} = D \nabla^2 \Psi(\underline{R}, t) + [E_T - V(\underline{R})] \Psi(\underline{R}, t) \quad (1)$$

we see that it may be interpreted as a generalized diffusion equation. The first term on the right-hand-side is the ordinary diffusion term, while the second term is a position-dependent rate (or branching) term. For an electronic system, $D = \hbar^2 / 2m_e$, \underline{R} is the three-N dimensional coordinate vector of the N electrons, and $V(\underline{R})$ is the Coulomb potential. Since diffusion is the continuum limit

of a random walk, one may simulate Eq. (1) with the function Ψ (note, *not* Ψ^2) as the density of "walks". The walks undergo an exponential birth and death as given by the rate term. This connection between a quantum system and a random walk was first noted by Metropolis, who attributes it to Fermi¹⁵.

The steady-state solution to Eq. (1) is the time-independent Schrödinger equation. Thus we have $\Psi(\underline{R}, t) \rightarrow \varphi(\underline{R})$, where φ is an energy eigenstate. The value of E_T at which the population of walkers is asymptotically constant gives the energy eigenvalue. Early calculations employing Eq. (1) in this way were done by Anderson on a number of one- to four-electron systems⁹.

Unfortunately, in order to treat systems larger than two electrons, the Fermi nature of the electrons must be taken into account. The antisymmetry of the eigenfunction implies that Ψ must change sign; however, a density (e.g. of walkers) cannot be negative. To handle this, Anderson made simplifying assumptions about the positions of the nodes. His method is *ad hoc*, and not readily generalizable. Another method which imposes the antisymmetry, and at the same time provides more efficient sampling (thereby reducing the statistical "noise"), is importance sampling with an antisymmetric trial function Ψ_T (see e.g. Ref. 8). The zeroes (nodes) of Ψ_T become absorbing boundaries for the diffusion process, which maintains the antisymmetry. The additional boundary condition that Ψ vanish at the nodes of Ψ_T is the fixed-node approximation. The magnitude of the error thus introduced depends on the quality of the *nodes* of $\Psi_T(\underline{R})$, and vanishes as Ψ_T approaches the true eigenfunction. To the extent that Ψ_T is a good approximation of the wave function, the true eigenfunction is almost certainly quite small near the nodes of Ψ_T . Thus one expects the fixed-node error to be small for reasonable choices of Ψ_T . Work on a number of systems has borne this out^{8,9,11}. In addition, this error is variationally bounded.

To implement importance sampling and the fixed-node approximation, Eq. (1) is multiplied on both sides by Ψ_T , and rewritten in terms of the new probability density $f(\underline{R}, t) = \Psi_T(\underline{R})\Psi(\underline{R}, t)$. The resultant equation for $f(\underline{R}, t)$ may be

written

$$\frac{\partial f}{\partial t} = D\nabla^2 f + [E_T - E_L(\mathbf{R})]f - D\nabla \cdot [f F_Q(\mathbf{R})] . \quad (2)$$

The local energy $E_L(\mathbf{R})$, and the "quantum force" $F_Q(\mathbf{R})$ are simple functions of Ψ_T given by

$$E_L(\mathbf{R}) \equiv H\Psi_T(\mathbf{R}) / \Psi_T(\mathbf{R}) , \quad (3a)$$

and

$$F_Q(\mathbf{R}) \equiv 2\nabla\Psi_T(\mathbf{R}) / \Psi_T(\mathbf{R}) . \quad (3b)$$

Equation (2), like Eq. (1) is a generalized diffusion equation, though now with the addition of a drift term due to the presence of F_Q .

In order to perform the random walk implied by Eq. (2) we use a short-time approximation to the Green's function which is used to evolve $f(\mathbf{R}, t) \rightarrow f(\mathbf{R}', t + \tau)$. This process is iterated to large t . Such an approach becomes exact in the limit of vanishing time-step size, τ .

Progress During Current Year

(1) We have developed a method of improving an importance function through an iterated use of wave-function scaling. For use in QMC one wants a trial function which is as simple as possible, since it will require repeated evaluation at each step of the random walk. Yet one wants a function which provides accurate results. In principle, since QMC solves the Schrödinger equation, one should obtain accurate results *regardless* of the choice of Ψ_T . However, as we noted already, for Fermi systems inaccurate nodes in Ψ_T will lead to a small error when the fixed-node approximation is used. Furthermore, the statistical "noise" will be large for a poor choice of Ψ_T .

We have found in our work^{8,11} that a *single determinant* Ψ_T with only a double-zeta basis set places the nodes extremely well as determined by the quality of the computed total energies. Increasing the basis set beyond double zeta appears to offer insignificant gain in either accuracy (i.e. the fixed-node error does not noticeably decrease) or precision (the statistical uncertainty, for

equal computing time, remains essentially unchanged). In practice we have included an electron-electron Jastrow factor in our functions Ψ_T in order to reduce statistical fluctuations, and in some cases we have also included an electron-nuclear factor. Neither factor affects the positioning of the nodes, and hence the fixed-node energies.

Since the fixed-node QMC approach involves an approximation in the placement of the nodes, and, in addition, in many applications the statistical uncertainty needs to be further reduced, we have developed an iterative approach for globally (rather than locally) performing this correction.

Note first that the additional boundary condition that the eigenfunction vanish at the nodes of Ψ_T will generally give a solution which fails to satisfy the virial theorem. Thus the fixed-node expectation value of V is not exactly $-2T$. (Here we assume an equilibrium geometry.) We may therefore consider the fixed-node eigenfunction, which we shall denote $\hat{\varphi}(\{\mathbf{r}_i\})$, as a variational function which may be further optimized by scaling¹⁶. In our notation, the caret indicates that $\hat{\varphi}$ carries the fixed-node constraint, and $\{\mathbf{r}_i\}$ indicates the set of *all* coordinates.

Let us define

$$V(1) \equiv \langle \hat{\varphi}(\{\mathbf{r}_i\}) | V | \hat{\varphi}(\{\mathbf{r}_i\}) \rangle . \quad (4a)$$

$$T(1) \equiv \langle \hat{\varphi}(\{\mathbf{r}_i\}) | T | \hat{\varphi}(\{\mathbf{r}_i\}) \rangle . \quad (4b)$$

and the scaled quantities $V(\eta)$ and $T(\eta)$ analogously in terms of the scaled function $\hat{\varphi}(\eta\{\mathbf{r}_i\})$. The expressions in Eq. (4) must of course be divided by $\langle \hat{\varphi}(\{\mathbf{r}_i\}) | \hat{\varphi}(\{\mathbf{r}_i\}) \rangle$ if $\hat{\varphi}$ is not normalized. It is readily established that $V(\eta) = \eta V(1)$ since the Coulomb potential scales as $1/r$. Similarly, $T(\eta) = \eta^2 T(1)$ since ∇^2 scales as $1/r^2$. Combining these expressions one obtains

$$E(\eta) = \eta V(1) + \eta^2 T(1) \quad (5)$$

Varying Eq. (5) with respect to η minimizes $E(\eta)$ at

$$\eta = -V(1)/2T(1) \quad (6a)$$

and

$$E(\eta) = -V(1)^2 / 4T(1) \quad (6b)$$

Thus the function $\hat{\varphi}(\eta\{\mathbf{r}_i\})$ has a lower variational energy than $\hat{\varphi}(\{\mathbf{r}_i\})$, and in addition satisfies the virial theorem since $-V(\eta)/2T(\eta) = -\eta^{-1}V(1)/2T(1) = 1$. Note that the global scaling has uniformly expanded or contracted the nodal surfaces originally present in Ψ_T . As we demonstrate below, these new nodes are better than the original nodes of Ψ_T . However, $\hat{\varphi}(\eta\{\mathbf{r}_i\})$ is no longer an eigenfunction of the Schrödinger equation. Thus we may iterate the above procedure starting with the new nodes--i.e. using¹⁷ a Ψ_T whose nodes are those of $\hat{\varphi}(\eta\{\mathbf{r}_i\})$ (see Fig. 1). Such a function, $\Psi_T^{(1)}$, may be obtained by replacing all coordinates $\{\mathbf{r}_i\}$ in Ψ_T by $\eta\{\mathbf{r}_i\}$. (Essentially this involves scaling all the orbital exponents and the inter-atomic separations.) Now starting with $\Psi_T^{(1)}$ the QMC method converges to an eigenstate $\hat{\varphi}^{(1)}(\eta\{\mathbf{r}_i\})$. Because $\hat{\varphi}^{(1)}(\eta\{\mathbf{r}_i\})$ has the same nodes as $\hat{\varphi}(\eta\{\mathbf{r}_i\})$, $\hat{\varphi}^{(1)}$ must have the lower energy since it is the exact solution for these nodes. Again, due to the fixed-node boundary condition with the new nodes, the virial theorem may not be satisfied, resulting in $\eta' = -V/2T \neq 1$ (for $\hat{\varphi}^{(1)}$). Thus we rescale by η' to obtain $\hat{\varphi}^{(1)}(\eta'\eta\{\mathbf{r}_i\})$, which has a lower variational energy and again satisfies the virial theorem. The expanded or contracted nodes may then be fed back into a $\Psi_T^{(2)}$ and the process repeated. It is expected that the sequence $\eta, \eta', \eta'', \dots$ rapidly converges to unity, so that no appreciable gains will be obtained beyond the first few iterations. Figure 1 gives a schematic illustration of this iterative procedure. Since the fixed-node energies for the sequence of functions $\hat{\varphi}(\{\mathbf{r}_i\}), \hat{\varphi}^{(1)}(\eta\{\mathbf{r}_i\}), \hat{\varphi}^{(2)}(\eta'\eta\{\mathbf{r}_i\}) \dots$ is of decreasing energy, the nodes improve upon scaling.

(2) We have calculated the energy of the first excited state of methylene¹⁸ in order to obtain the (until recently) elusive singlet-triplet splitting. This is the first QMC calculation of an excited state. Our results are in excellent agreement with the most recent experiments.

Also, as shown in Table I, the QMC total energies for both the singlet and the triplet states of methylene compare favorably with CI calculations. For the best

trial function used, the *total energy* is correct to better than 0.008 h (5 kcal/mole) of experiment, or to 1 part in 5000. The statistical uncertainty is roughly half this value (2-2.5 kcal/mole). The remaining error may be attributed to the fixed-node and the short-time approximations. This translates to a Monte Carlo accuracy of 99.98% of the total energy and 96-98% of the correlation energy. Therefore in the present application, where the time-step error is negligible, the fixed-node error is seen to be manageably small. Furthermore, to within 1 kcal/mole, this error is the same for the two states. This means not only that the absolute error is small, but that there is also a large degree of cancellation of this error in evaluating the energy gap. In fact, for the energy gap the error is considerably less than the statistical uncertainty.

To obtain our best estimate for T_0 , we calculated a weighted average of the energy differences for our various trial functions. Our final result is $T_0 = 9.4 \pm 2.2$ kcal/mole. This result is in excellent agreement with the recent experimental results of McKellar *et al*²⁴.

(3) We have calculated points along the reaction path of the H + H₂ exchange reaction. Particular emphasis has been placed on the saddle point, for which Liu²⁵ has performed the most extensive CI calculation to date. Nevertheless, the bound for the barrier height which we obtained²⁶ by QMC is 0.16 kcal/mole below Liu's bound (see Table II), and probably lies within 0.1 kcal/mole of the exact answer. In addition, we were able to obtain these results with only single-determinant trial functions, and a basis set expansion at only the double-zeta level.

The nodes, which are so important in determining the correct energy, prove to be quite insensitive to basis set after the double zeta level. A single-zeta basis set, however, gives a very poor nodal description (see Figs. 2-4).

(4) Monte Carlo, as alluded to earlier, is such a computationally intensive activity that new techniques are needed if one wishes to attack large systems or

obtain very high precision (e.g. better than 99.99%). One avenue we have explored, in collaboration with the Advanced Computer Architecture Laboratory at LBL, is the use of parallel computing architectures. Briefly, we have found that Monte Carlo can be readily made to run at 95% efficiency on an 8 processor system. With sufficient memory, precision will scale as the square root of the number of processors, while computing time for a fixed precision, will scale inversely almost linearly with processors. We explored several different directions for parallelizing QMC, as well as load-balancing techniques to keep the efficiency near 100%.

(5) An accurate calculation of the binding energy of N_2 has been a classically difficult problem using traditional *ab initio* quantum chemical approaches. Since the quantity of interest, $E_{binding}$, is desired to better than 5 kcal/mole out of a total energy (for N_2) of over 68,000 kcal/mole, this is an example where QMC requires very high precision. Thus we have performed this calculation on the experimental parallel processing system mentioned above. We have obtained the N_2 binding energy to be 233 ± 5 kcal/mole. To within the statistical uncertainty, this answer agrees with experiment.

(6) We have also begun investigating the electron affinity of F, since affinities are generally difficult by traditional approaches. In addition, we are exploring some new directions. As mentioned in the previous section, molecular pseudopotentials hold promise for simplifying Monte Carlo calculations. Little loss of accuracy is anticipated. However, this must be explored. More importantly, one must learn how to translate angular momentum dependent "effective-core-potentials" into a form applicable to QMC. Another direction we are following is the explicit calculation of derivatives by Monte Carlo. This would enable direct calculation of forces and more accurate determination of potential-energy surfaces. Also, this would provide the ability to find equilibrium geometries.

List of Manuscripts

1. "Quantum Monte Carlo Study of the Classical Barrier Height for the $H + H_2$ Exchange Reaction: Restricted *versus* unrestricted trial functions"
P. J. Reynolds, R. N. Barnett, and W. A. Lester, Jr., *Int. J. Quant. Chem., Chem. Symp.* 18,xxx (1984).
2. "Quantum Monte Carlo Calculation of the Singlet-Triplet Splitting in Methylene" P. J. Reynolds, M. Dupuis, and W. A. Lester, Jr., *J. Chem. Phys.* accepted.
3. "Fixed-node Quantum Monte Carlo Study of the Classical Barrier Height for the $H + H_2$ Exchange Reaction" R. N. Barnett, P. J. Reynolds, and W. A. Lester, Jr., *J. Chem. Phys.* submitted.

References

1. M. H. Kalos, Phys. Rev. 128, 1791 (1962); J. Comp. Phys. 1, 257 (1967).
2. M. H. Kalos, D. Levesque, and L. Verlet, Phys. Rev. A 9, 2178 (1974).
3. J. B. Anderson, J. Chem. Phys. 63, 1499 (1975); 65, 4121 (1976).
4. D. M. Ceperley and M. H. Kalos, in *Monte Carlo Methods in Statistical Physics*, edited by K. Binder (Springer-Verlag, Berlin, 1979).
5. J. B. Anderson, J. Chem. Phys. 73, 3897 (1980); F. Mentch and J. B. Anderson, J. Chem. Phys. 74, 6307 (1981).
6. D. M. Ceperley and B. J. Alder, Phys. Rev. Lett. 45, 566 (1980).
7. D. M. Ceperley in *Recent Progress in Many-Body Theories*, edited by J. G. Zabolitzky, M. de Llano, M. Fortes, and J. W. Clark (Springer-Verlag, Berlin, 1981).
8. P. J. Reynolds, D. M. Ceperley, B. J. Alder, and W. A. Lester, Jr., J. Chem. Phys. 77, 5593 (1982).
9. J. W. Moskowitz, K. E. Schmidt, M. A. Lee, and M. H. Kalos, J. Chem. Phys. 7, 349 (1982).
10. D. M. Ceperley, J. Comp. Phys. 51, 404 (1983).
11. P. J. Reynolds, R. N. Barnett, and W. A. Lester, Jr., Int. J. Quant. Chem. Symp. 18, xxx (1984); F. Mentch and J. Anderson, J. Chem. Phys. 80, 2875 (1984); R. N. Barnett, P. J. Reynolds, and W. A. Lester, Jr., J. Chem. Phys., *submitted*.
12. D. M. Ceperley and B. J. Alder, J. Chem. Phys., *in press*.
13. K. E. Schmidt and M. H. Kalos, in *Monte Carlo Methods in Statistical Physics II*, edited by K. Binder, *to be published*.
14. B. Holmer and D. M. Ceperley, *private communication*; B. Wells, P. J. Reynolds, and W. A. Lester, Jr., *unpublished*.
15. N. Metropolis and S. M. Ulam, J. Am. Stat. Assoc. 44, 335 (1949).
16. P-O. Löwdin, in *Advances in Chemical Physics*, Vol. II, edited by I. Prigogine (Interscience, New York, 1959); E. A. Hylleraas, Z. Physik 54, 347 (1929).

17. In principle we would continue the iteration with $\hat{\varphi}(\eta\{\tau_i\})$ directly, except that we have no analytic expression for this function.
18. P. J. Reynolds, M. Dupuis, and W. A. Lester, Jr., J. Chem. Phys. to be published.
19. D. Feller, L. E. McMurchie, W. T. Borden, and E. R. Davidson, J. Chem. Phys. 77, 6134 (1982).
20. J. H. Meadows and H. F. Schaefer III, J. Am. Chem. Soc. 98, 4383 (1976).
21. P. Saxe, H. F. Schaefer III, and N. C. Handy, J. Phys. Chem. 85, 745 (1981).
22. H.-J. Werner and E.-A. Reinsch, J. Chem. Phys. 76, 3144 (1982);
23. E. R. Davidson, L. E. McMurchie, and S. Day, J. Chem. Phys. 74, 5491 (1981).
24. A. R. W. McKellar, P. R. Bunker, T. J. Sears, K. M. Evenson, R. J. Saykally, and S. R. Langhoff, J. Chem. Phys. 79, 5251 (1983).
25. B. Liu, J. Chem. Phys. 80, 581 (1984).
26. R. N. Barnett, P. J. Reynolds, and W. A. Lester, Jr., J. Chem. Phys. submitted.
27. D. M. Ceperley and B. J. Alder, J. Chem. Phys. to be published.

Table Captions

Table I. Comparison of QMC results on methylene with SCF, CI, and experimental values. The results indicated as "expt" are corrected for zero-point motion and relativistic effects to make the comparison direct. The lowest variance QMC result for T_0 is not the difference of the QMC values given for the two states. Instead T_0 is obtained by averaging the results of all the Ψ_T 's we used in this study.

Table II. Comparison of computed reaction barrier heights for the $H + H_2$ exchange reaction. Fixed-node quantum Monte Carlo provides an excellent bound, which is better than that given by CI, and is within 0.1 kcal/mole of the exact value.

Table I.

Method*	Energy (hartrees)		T_0 (Kcal/mole)
	3B_1	1A_1	
SCF	-38.9348 ^a	-38.8944 ^b	25.4
2C-SCF	—	-38.9177 ^c	10.7 ^d
2R-CI-SD	-39.1160 ^e	-39.1003 ^e	9.9 ^e
CI-SD(Q)	-39.122 ^c	-39.105 ^c	10.7 ^c
QMC	-39.140(4)	-39.128(3)	9.4(2.2)
"expt"	-39.148 ^f	-39.133 ^g	9.55 ^h

* Glossary of Methods

SCF = self-consistent field

2C-SCF = two-configuration SCF

2R-CI-SD = two-reference configuration, single and double excitations CI for the singlet; one reference configuration CI-SD for the triplet.

CI-SD(Q) = singles and doubles CI, quadruples estimated.

QMC = quantum Monte Carlo (this work).

^a Ref. 19,20.

^b Ref. 21.

^c Ref. 19.

^d using 1C-SCF for the 3B_1 state.

^e Ref. 22.

^f Ref. 23.

^g obtained by subtracting T_0 from the "expt" energy of 3B_1 CH₂.

^h obtained from T_0 of McKellar *et. al.* (Ref. 24), corrected for zero-point motion and relativistic effects.

Table II

Method	E_b
Best CI ^a	< 9.86 $\approx 9.59 \pm 0.06$
FNQMC (present work)	< 9.70 (0.13)
Exact ^b	9.65 (0.08)

^a Ref. 25.

^b Ref. 27.

Figure Captions

Figure 1. Schematic illustration of process for globally optimizing Ψ_T . The original trial function is $\Psi_T(\{r_i\})$, while the subsequent trial functions are $\Psi_T^{(1)}$, $\Psi_T^{(2)}$, etc. The functions in the middle column are the solutions of the fixed-node Schrödinger equation, with the nodes of the Ψ_T to the left. The final functions on the right are the scaled fixed-node functions, but these are no longer solutions to the Schrödinger equation. Along the path indicated by arrows, each function has a lower variational energy than that preceding it.

Figure 2. Exchange nodes of a single-zeta quality trial function. The circles represent the hydrogen nuclei. The curves are cross sections through a selection of nodal surfaces arising from the exchange antisymmetry. Full nodal surfaces may be obtained by rotating the curves around the internuclear axis. Each surface is obtained by fixing the position of one electron on it and finding the locus of points for the other like-spin electron at which the trial function vanishes. It can easily be shown that the trial function is zero whenever both like-spin electrons are *anywhere* on this surface. Distances are in bohr.

Figure 3. Exchange nodes for a double-zeta quality trial function. See Fig. 2 for further explanation of this figure. Note how different these nodes are from those depicted in Fig. 2.

Figure 4. Exchange nodes for a near Hartree-Fock quality trial function. See Fig. 2 for further explanation of this figure. Note that approaching the basis-set limit has little effect on the nodes, past the single-zeta level.

$$\Psi_T(\{r_i\}) \xrightarrow{QMC} \tilde{\phi}(\{r_i\}) \xrightarrow{Scaling} \tilde{\phi}(\eta\{r_i\})$$



$$\Psi_T^{(1)}(\eta\{r_i\}) \rightarrow \tilde{\phi}^{(1)}(\eta\{r_i\}) \rightarrow \tilde{\phi}^{(1)}(\eta'\eta\{r_i\})$$



$$\Psi_T^{(2)}(\eta'\eta\{r_i\}) \rightarrow \tilde{\phi}^{(2)}(\eta'\eta\{r_i\}) \rightarrow \tilde{\phi}^{(2)}(\eta''\eta'\eta\{r_i\})$$



...

Fig. 1

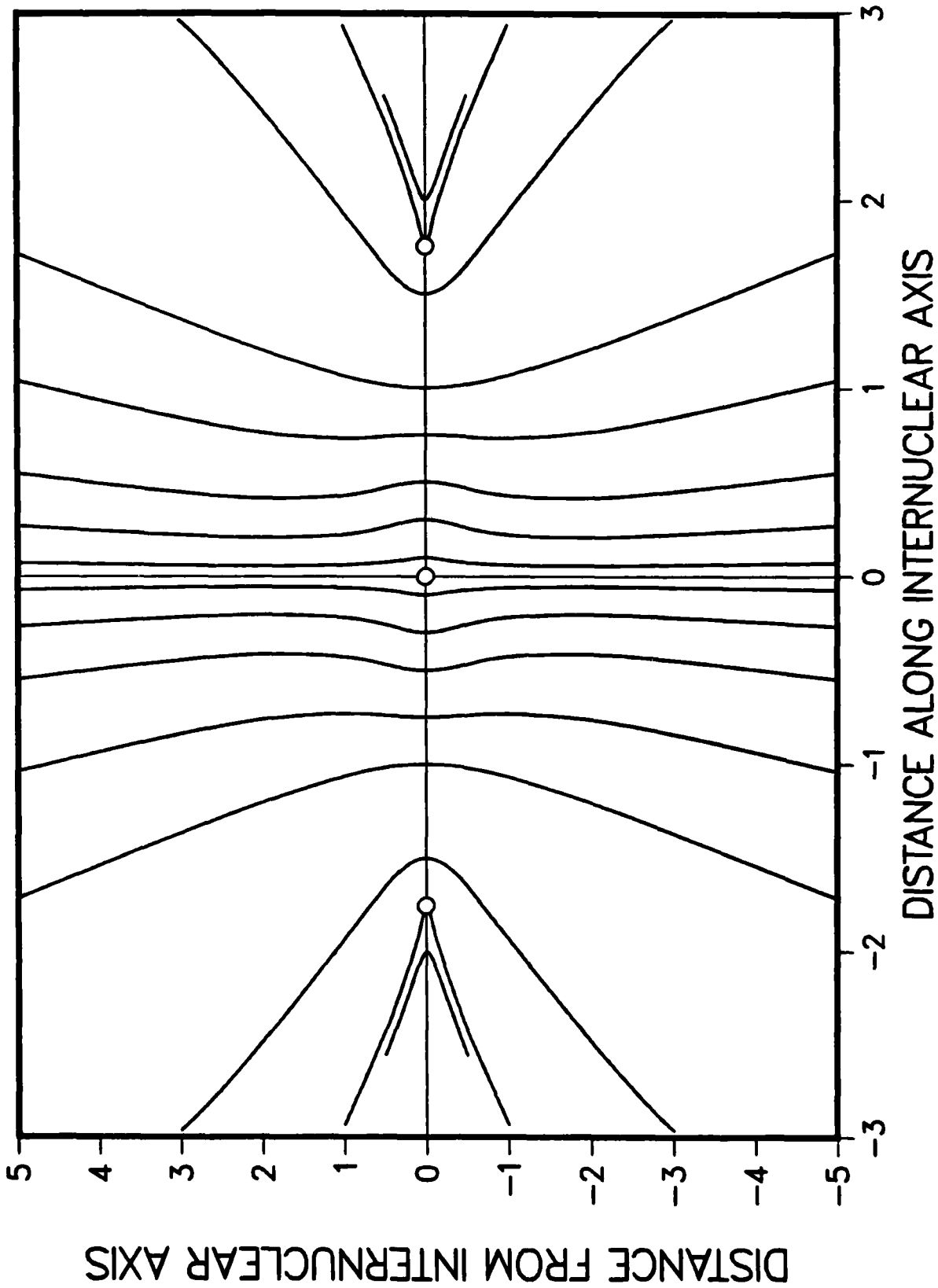


Fig. 2

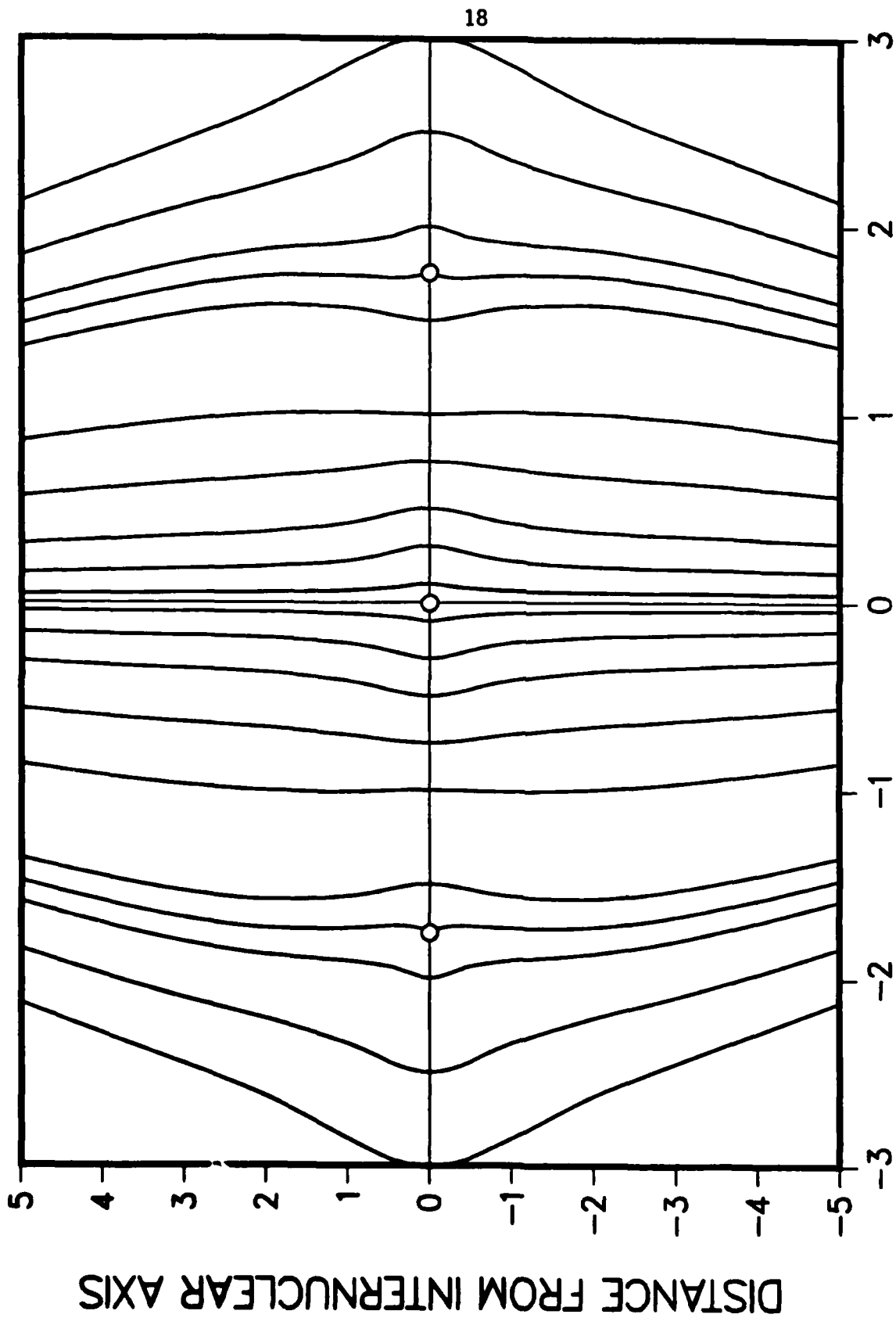


Fig. 3

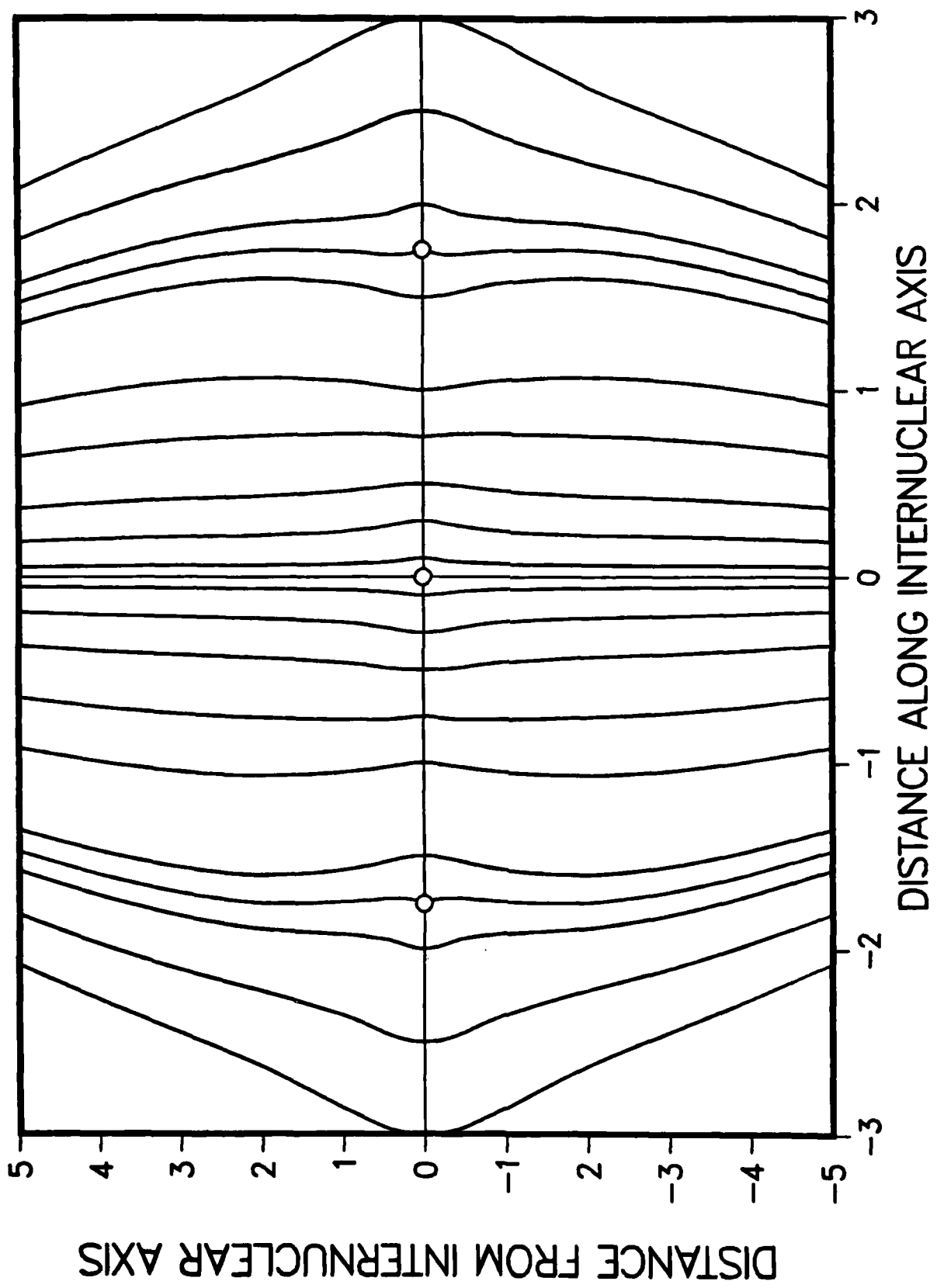


Fig. 4

END

FILMED

12-84

DTIC